CMS Physics Analysis Summary

Contact: cms-pag-conveners-susy@cern.ch 2009/07/13

Discovery potential and measurement of a dilepton mass edge in SUSY events at $\sqrt{s} = 10$ TeV

The CMS Collaboration

Abstract

Within the minimal supergravity model (mSUGRA), the observability of the decay of the next-to-lightest neutralino into leptons has been studied using the full simulation of the CMS detector. The final state signature consists of two opposite sign leptons, several hard jets and missing transverse energy. Using three different minimal supergravity benchmark points the possible discovery of a mSUGRA signal is studied. The expected precision of the measurement of the dileptonic mass edge is reported for 200 pb^{-1} and 1 fb^{-1} of data, including systematic and statistical uncertainties and comparing different decay signatures.

1 Introduction

The standard model of particle physics (SM) leads to a number of unsolved issues like the hierarchy problem and it provides no solution for pressing questions arising from astrophysical observations, most notably dark matter. In supersymmetry (SUSY) a natural candidate for dark matter can be found if R-parity conservation is assumed. Supersymmetric particles (sparticles) have not been observed up to now which implies that they have to be heavy. On the other hand to provide a solution to the hierarchy problem their masses have to be in the TeV range.

The long anticipated start of the Large Hadron Collider (LHC) in 2009 will allow to explore this new TeV range. With its center-of-mass energy of 10 TeV in 2010 it will allow to probe supersymmetric models very early on. A key point after discovery will be the determination of the sparticle properties. If R-parity is conserved the lightest neutralino escapes detection and no mass peaks can be observed in SUSY decay chains. Of special interest are robust signatures such as edges in mass distributions in leptonic final states which can be probed with the CMS experiment.

The purpose of this analysis is to observe a significant excess of opposite sign same flavour leptons over the various backgrounds and to measure the endpoint in the invariant mass distribution. All flavour symmetric background (including SUSY decays of this type) can be determined from data events with opposite sign opposite flavour leptons. The aim is to perform such an analysis already with the first LHC data which is expected to amount to roughly 200-300 pb^{-1} in 2010.

2 Signal

Three minimal supergravity benchmark points (Tab.1) have been studied to cover different decay modes of the neutralinos within supersymmetry. The mass spectra of the three benchmark points have been calculated using the SOFTSUSY code [1]. All branching ratios have been calculated with the SUSYHIT program [2] and the events are simulated using PYTHIA [3]. The k-factor for the cross section at 10 TeV is calculated using a modified version of PROSPINO 2 [4]. In mSUGRA there are very long decay chains leading to several hard jets. The escaping neutralino leads to missing transverse energy. This fact allows a search region to be defined to observe an excess over the SM and this determines the main event selection criteria as described in Sec. 4.

Table 1: mSUGRA benchmark points LM0, LM1 and LM9.

	m_0 [GeV]	$m_{1/2}$ [GeV]	A_0 [GeV]	$\tan\beta$	sign μ	σ_{LO} [pb]	σ_{NLO} [pb]	$m_{ll,max}$ [GeV]
LM0	200	160	-400	10	+1	110.0	151.8	52.7
LM1	60	250	0	10	+1	11.1	21.7	78.1
LM9	1450	175	0	50	+1	16.1	18.2	62.9

Additionally the leptonic decay of the next-to-lightest neutralino gives a characteristic signature. This decay can proceed in different ways even in the mSUGRA model. A mass difference of the neutralinos smaller than the Z boson mass and any slepton mass leads to a three body decay. In that case the endpoint in the lepton invariant mass represents directly the mass difference of the two lightest neutralinos

$$m_{ll,max} = m_{\tilde{\chi}_2^0} - m_{\tilde{\chi}_1^0}. \tag{1}$$

The shape of the distribution depends strongly on the mSUGRA parameters [5]. If the sleptons are heavy (LM9) the decay with a virtual Z boson exchange dominates and the endpoint is peaked towards the Z boson mass. If the sleptons are light they can drastically change the shape of the distribution leading to a destructive interference at the endpoint. The interpretation of a leptonic endpoint is therefore challenging especially with a small amount of events.

A two-body decay occurs via a real slepton and is allowed if at least one slepton is lighter than the mass difference of the neutralinos. In that case the endpoint can be expressed by

$$(m_{ll}^{max})^2 = \frac{\left(m^2_{\tilde{\chi}^0_2} - m^2_{\tilde{l}}\right)\left(m^2_{\tilde{l}} - m^2_{\tilde{\chi}^0_1}\right)}{m^2_{\tilde{l}}}, \tag{2}$$

where $m_{\tilde{l}}$ is the mass of the intermediate slepton. The shape of the mass edge results only from kinematics and is triangular. At LM0 the 3-body decay mode is present as for LM9, while at LM1 the 2-body decay is possible as shown in App. A for the three LM benchmark points at parton level.

If the mass difference matches the Z boson mass this leads to an enhanced Z boson production accompanied by large missing transverse energy and several hard jets. This signature is not in the focus of the present analysis. It has been studied for example in [6]. Another possibility in mSUGRA is a decay predominantly through the lightest Higgs boson which leads to a different signature as well.

3 Physics objects

The datasets with a vector boson or a $t\bar{t}$-pair have been simulated using the MADGRAPH matrix element generator [7]. The parton shower and hadronisation is modelled in PYTHIA. The di-jet, quarkonia, Wγ and Zγ samples are simulated using PYTHIA. All samples undergo the full CMS detector simulation. The Monte Carlo (MC) production was targeted of an integrated luminosity of 200 pb^{-1} and used ideal calibration and alignment constants.

The samples have been scaled to next-to-leading order cross sections. For the SUSY samples the k-factor calculated with PROSPINO 2 has been used. The k-factor for the $t\bar{t}$ sample of 1.3 has been derived from [8]. The k-factors of the Z+jets and the W+jets samples of 1.14 have been derived from [9]. For the di-jet sample no k-factors are applied.

Muon identification requires reconstruction in both the muon system and the inner tracker [10]. The track of the muon in the inner tracker has to have at least 11 hits and the χ^2/ndf of the global track fit has to be below 10. Additionally a $p_T > 10$ GeV and $|\eta| < 2$ is required for each muon. The impact parameter of the muon track which is corrected for the beam-spot position is required to be below 2 mm and this cut could be tightened if necessary (the current set of events does not include misalignment so a too tight cut could overestimate the efficiency in real data).

Each electron has to fulfill the tight electron identification criteria, which consist of a set of cuts depending on the electron p_T and η [11]. Additionally a $p_T > 10$ GeV and $|\eta| < 2$ is required for each electron. The impact parameter of the electron track which is corrected for the beam-spot position is required to be below 2 mm as in the muon case.

A combined relative lepton isolation has been used. The isolation uses information from both calorimeters and the silicon tracker. The isolation value (Iso) is given by the ratio of the sum of all (subtracting the lepton) E_T or p_T objects within a cone in η-ϕ-space of $\Delta R = \sqrt{\Delta\eta^2 + \Delta\phi^2} <$

0.3 around the lepton and the lepton p_T. It has been calculated using

$$Iso = \frac{\sum_{ECAL} E_T + \sum_{HCAL} E_T + \sum_{tracks} p_T}{p_T} \quad (3)$$

where the first sum runs over transverse energy in the electromagnetic calorimeter, the second sum runs over the transverse energy in the hadronic calorimeter and the third sum runs over the transverse momentum deposited in the tracker within the cone subtracting the lepton.

The isolation for muons and electrons is shown in App. B. The cut value is chosen to be $Iso < 0.2$ for muons and the cut is placed at $Iso < 0.4$ for electrons, to obtain a similar rejection and efficiency for electrons and muons down to low p_T.

The jet algorithm is a seedless infrared safe cone algorithm (SIScone) [12] with a cone size of 0.5 in ΔR. The jets are corrected using MC jet energy corrections [13]. Each corrected jet is required to have a $p_T > 50$ GeV and the jet axis has to be within $|\eta| < 2.5$. This tight η cut would allow us to include tracker information if necessary and not to rely on the hadronic calorimeter only. Additionally the overlap of the jets with the electrons is checked and a jet is vetoed if an electron close to the jet is found. The missing transverse energy (MET) is based on the calorimeter information and is corrected for muon energy deposition and jet energy scale [14].

3.1 Efficiency correction

Since the muon and electron reconstruction efficiencies are not equal these efficiencies have to be measured from data. Therefore a "tag and probe" method using events with a Z boson can be used. To select clean Z events a tight selection is applied to one lepton (tag) and only loose criteria are used on the probe side. A study of a "tag and probe" method is presented in [15].

We use the lepton efficiencies ϵ to correct the invariant mass distributions of the lepton pairs. Each lepton in the distributions is weighted by $1/\epsilon$ depending on its η and p_T.

The efficiency in SUSY or $t\bar{t}$ events is lower than in events with a Z boson (due to the more crowded events). Additionally the efficiency cannot be measured to a ultimate precision especially at low p_T and high jet multiplicity. Therefore we assume a p_T dependent systematic uncertainty on the lepton efficiency varying from 20% for a p_T below 20 GeV to 5% at a p_T above 100 GeV. This tests the robustness of the analysis against uncertainties in the lepton reconstruction and identification efficiency.

4 Event selection

The base selection requires two leptons of opposite sign. We do not require two same flavour leptons in order to measure the background events directly from the same dataset as described in Sec. 4.1. To stay above the trigger treshold the first lepton is required to have a $p_T > 16$ GeV. The main SUSY selection is based on jets and missing transverse energy. The cuts have not been optimised at a certain benchmark point, but should reflect the general SUSY signature. The selection requires three jets with $p_T^{j1} > 100$ GeV, $p_T^{j2} > 50$ GeV, and $p_T^{j3} > 50$ GeV. Additionally a missing transverse energy of at least 100 GeV is required.

In this analysis we require that at least one of two single leptonic high level trigger (HLT) conditions, electron or muon, is satisfied. Since the leptons originating from the signal decay have a very soft p_T spectrum we use the triggers with the lowest available threshold for electrons (15 GeV) and muons (11 GeV).

Due to the SUSY signature of hard jets and missing transverse energy there exists the possibility to use a single hadronic trigger to recover possible inefficiencies of the leptonic triggers and we compare their efficiencies to hadronic trigger efficiencies.

We observe an efficiency (in the inclusive SUSY sample) of $96.1 \pm 0.5\%$ for the isolated leptonic paths with respect to the final event selection. The most efficient hadronic trigger yields an efficiency of $97.9 \pm 0.4\%$ using the single jet trigger with a threshold of 110 GeV.

Table 2: Number of selected events using the described event selection for an integrated luminosity of 200 pb^{-1}. The row LM0 signal refers to events where the signal decay is present.

	σ_{LO} [pb]	k-factor	HLT	≥ 2 leptons	≥ 3 jets	MET
LM0 signal	1.0	1.38	362	226	129	87
LM0 inclusive	110.0	1.38	8161	1007	543	362
tt+jets	319.0	1.3	25655	2411	238	80
Z+jets	3700.0	1.14	622956	199773	510	1
W+jets	40000.0	1.14	3108397	298	5	2
Diboson	51.9	1.0	5444	885	2	0
Di-jets	2003572.9	1.0	2801134	560	4	0

The number of events obtained after each cut is listed in Tab. 2. After HLT selection the sample is still dominated by di-jet and W events. The requirement of two isolated and well identified opposite sign leptons rejects most of the di-jet events and the selection is dominated by events with a Z boson. After requirement of three hard jets a SUSY inclusive signal to background ratio of roughly one can be reached. After requirement of missing transverse energy the main background from the standard model consists of $t\bar{t}$-events. With the described selection an efficiency of 25% on the signal events is obtained. At the studied benchmark point LM0 a high number of SUSY background events is found (flavour symmetric background from chargino decays) which is irreducible. This complicates the discovery of this decay at this point as described in Sec. 5.3.

4.1 Statistical measurement of the background events

All background which leads to uncorrelated lepton pairs can be measured directly from data [16]. Therefore we select the opposite sign opposite flavour lepton pairs and use this distribution to extrapolate to the same flavour opposite sign lepton pair distribution.

With this method one is able to predict all backgrounds which produce uncorrelated leptons such as W, $t\bar{t}$, di-jet and WW events.

The invariant mass distribution of all opposite sign same flavour leptons for 200 pb^{-1} is shown in Fig. 1(a). To obtain the pseudo data in this plot no scaling has been applied but only the number of expected events in 200 pb^{-1} has been analysed. The opposite sign opposite flavour distribution used to extrapolate the background is displayed in Fig. 1(b). One can see that at a low luminosity the statistical fluctuations are relatively large. Therefore the background is modelled and fitted as described in Sec. 5.

5 Determination of the mass edge

The model used for the fit of the mass edge consists of three parts. To model the signal the theoretical model [5, 17] convoluted numerically with a gaussian has been used in case of a

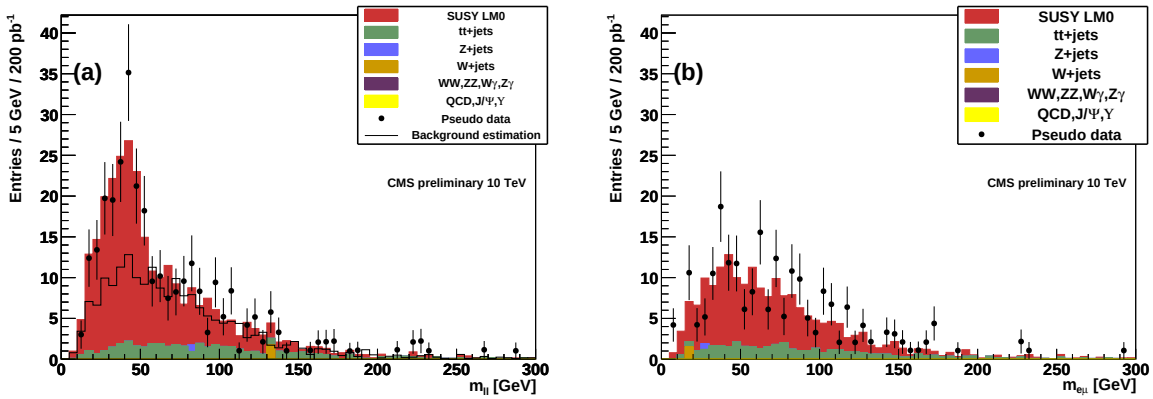

Figure 1: The same flavour opposite sign lepton pair distribution including all cuts is shown in (a). The black solid line represents the extrapolation from (b), which displays the opposite flavour opposite sign lepton pairs. The black points represent psuedo data of one experiment where no scaling has been applied but exactly 200 pb^{-1} of MC events have been analysed.

3-body decay

$$S(m_{ll}) = \frac{1}{\sqrt{2\pi}\sigma} \int_0^{m_{cut}} dy \cdot y \frac{\sqrt{y^4 - y^2\left(m^2 + M^2\right) + \left(m\,M\right)^2}}{\left(y^2 - m_Z^2\right)^2} \tag{4}$$

$$\times \left(-2y^4 - y^2\left(m^2 + 2M^2\right) + \left(m\,M\right)^2\right) e^{\frac{-\left(m_{ll}-y\right)^2}{2\sigma^2}}, \tag{5}$$

where $m = m_{\tilde{\chi}_2^0} - m_{\tilde{\chi}_1^0}$ is the sum, $M = m_{\tilde{\chi}_2^0} + m_{\tilde{\chi}_1^0}$ is the difference in neutralino mass and M_Z is the Z mass, which is kept fixed. This neglects the masses of the leptons in the final state and includes only the Z boson contribution to the decay. It is therefore a good approximation at LM9 where the sleptons are very heavy, while the approximation at LM0 is not as good.

In case of the two-body decay the signal model consists of a triangle convoluted with a gaussian

$$T(m_{ll}) = \frac{1}{\sqrt{2\pi}\sigma} \int_0^{m_{cut}} dy \cdot y e^{\frac{-\left(m_{ll}-y\right)^2}{2\sigma^2}}. \tag{6}$$

The decision as to which function is fitted to the same flavour opposite sign invariant mass distribution can be based on a "goodness of fit" (χ^2) test. A curve parametrized as

$$B(m_{ll}) = m_{ll}^a \cdot e^{-b \cdot m_{ll}} \tag{7}$$

has been used to fit the opposite sign opposite flavour invariant mass distribution. Additionally the Z peak is fitted using a Breit-Wigner convoluted with a gaussian.

The fits are performed within the RooFit package [18] based on an unbinned and extended maximum likelihood fit to the di-lepton invariant mass distribution for both electrons and muons

$$L = \frac{e^{-\left(N_{Sig}+N_{Bkg}+N_Z\right)}}{\left(N_{Sig}+N_{Bkg}+N_Z\right)!} \prod_i \left[N_{Sig} P_S\left(m_{ll}\right)_i + N_{Bkg} P_B\left(m_{ll}\right)_i + N_Z P_Z\left(m_{ll}\right)_i\right]. \tag{8}$$

Here $P_S = S$ or $P_S = T$ is the signal probability density function (triangle or 3-body model convolved with a gaussian), P_B is the background model and P_Z is the Breit-Wigner function

convoluted with a gaussian. The number of signal N_{Sig}, background N_{Bkg} and Z events N_Z are fitted as well.

We fit this functions simultaneously to the ee, $\mu\mu$ (signal plus background model) and $e\mu$ (background model) invariant mass distributions.

5.1 Resolution measurement

The resolution smearing of the detector, which is used in the fit function (Eq. 4+6), is measured from Z events. The selection using two well identified opposite sign leptons is used without any additional event selection cuts. In the two distributions for electrons and muons a bifurcated Gaussian (with different widths on each side of the mean)

$$G_{BF}\left(m_{ll}\right) = \begin{cases} \frac{1}{\sqrt{2\pi}\sigma_L} e^{\frac{-\left(m_{ll}-m\right)^2}{2\sigma_L^2}} & m_{ll} \leq m \\ \frac{1}{\sqrt{2\pi}\sigma_R} e^{\frac{-\left(m_{ll}-m\right)^2}{2\sigma_R^2}} & m_{ll} > m \end{cases} \tag{9}$$

is fitted to account for the asymmetry in the distribution. The detector resolution is averaged from the two resolution values obtained from the fit subtracting the natural Z boson width. The values of the resolution parameter in the convolution is used in the final fit in Sec. 5.2. The fit of the resolution is shown in App. C and the values obtained are shown in Tab. 3.

Table 3: Resolution measurement from Z events.

	$\sigma_{\mu\mu}$	σ_{ee}
Resolution [GeV]	1.32 ± 0.07	2.02 ± 0.10

5.2 Fit of the mass edge for 200 pb^{-1} at LM0

Using all information derived up to this point one can perform a simultaneous fit to the invariant mass distributions of all opposite sign lepton pairs.

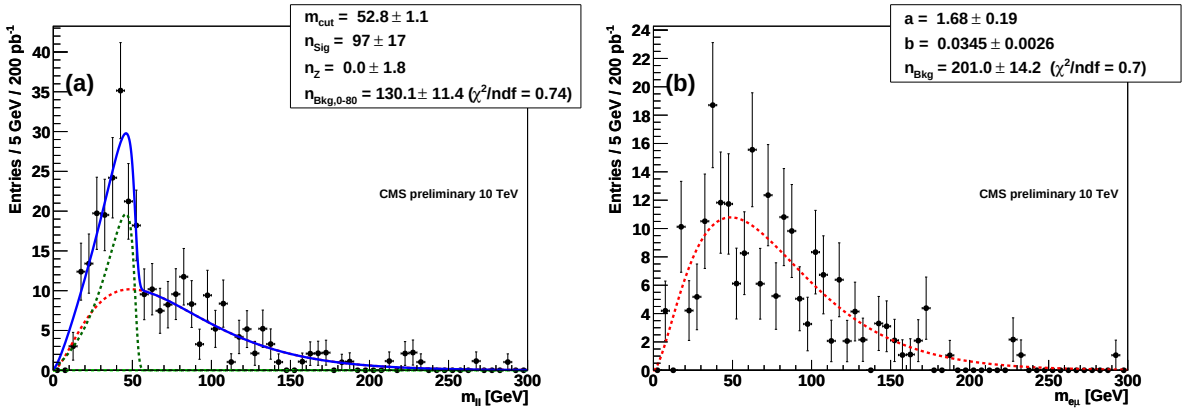

Figure 2: The combined fit at LM0 for 200 pb^{-1} is shown in (a). The green curve represents the SUSY signal model, the red curve is the background function and the light green dashed line the Z contribution. The black points represent the MC events. In (b) the fit of the background function to the $e\mu$ invariant mass distribution is shown.

The fit to the invariant mass distributions at LM0 for a dataset of exactly 200 pb^{-1} is shown in Fig. 2(a). To obtain a statistical interpretation we used the full statistic of the MC sample (2 fb^{-1}) scaled to 200 pb^{-1} and performed the fit. It yields a value of

$$m_{ll,max} = (51.3 \pm 1.5)\ \text{GeV}, \tag{10}$$

in case of the fit with the 3-body model ($\chi^2/\text{ndf} = 0.74$). If we fit the model for the two-body decay ($\chi^2/\text{ndf} = 0.79$) we obtain a value of

$$m_{ll,max} = (50.0 \pm 1.8)\ \text{GeV}, \tag{11}$$

The fact that one is not able to distinguish between the two- and the three-body decay makes the interpretation of an endpoint very difficult.

The derived number of signal events $n_{sig} = 97 \pm 17$ agrees with the number of signal events from MC truth (Tab. 2). The theoretical endpoint $m_{ll,theo} = 52.7$ GeV is reproduced in case of the fit with the three-body decay model, while we underestimate the theoretical value if we fit the model for a two-body decay.

The background fit of the opposite sign opposite flavour lepton pairs is shown in Fig. 2(b). We obtain a total number of background events of

$$n_{Bkg} = 201 \pm 14, \tag{12}$$

which is in agreement with the expected number from MC truth (192). The number of background events in the signal region from 0 to 80 GeV in m_{ll} yields a value of

$$n_{Bkg,0-80} = 130 \pm 11. \tag{13}$$

5.3 Significance

The significance at LM0 point has been calculated once including shape information and once from simple event counting. The significance is quoted for the signal decay only and not for a general SUSY excess over the Standard Model. The calculation of the signal significance including shape information (σ_{Shape}) uses signal and background probability density functions and the pseudo datapoints. We use the profile likelihood ratio as a test statistic and perform a fit with signal plus background hypothesis and a fit with the background only hypothesis given the pseudo datapoints. The p-Value (and significance) can then be constructed from the negative logarithm of the profile likelihood ratio.

This significance is compared to the calculation from the number of signal and background events only (σ_{Count}). The number of background events is determined by integration over opposite sign opposite flavour lepton pairs in the region between 0 and 80 GeV. The number of signal events is determined by integration over the same flavour opposite sign lepton pair events. Since the number of background events has been extrapolated from data the method Z_{Bi} described in [19] has been used to calculate the significance. Here we use a scaling factor $\tau = 1$ to predict the number of background events and calculate the excess of events over this background.

5.4 Systematic uncertainty of the significance

The main source for systematic uncertainties is the jet energy scale uncertainty. It is assumed to be 5% at an integrated luminosity of 200 pb^{-1} [13]. Due to the way the missing transverse

energy corrections are implemented it is anti-correlated with MET:

$$\vec{\not{E}}_T^{corr} = \vec{\not{E}}_T - \sum_{i=1}^{N_{jets}} \left[\vec{p}_{T_i}^{corr} - \vec{p}_{T_i}^{raw}\right]. \quad (14)$$

This correlation has been taken into account. All jets above the threshold of 30 GeV which do not overlap with an electron are shifted by $\pm 5\%$ in energy which propagates into the MET calculation.

Evaluating the uncertainty on the number of events due to the uncertainty of the jet energy scale one obtains the numbers shown in Tab. 4. The variation in the number of events leads to different observed significances in the experiment.

Table 4: Systematic uncertainties on the jet energy scale and their impact on the number of events at LM0.

JES	N_{Sig}	$N_{Bkg,0-80}$	N_{Bkg}	N_Z
0.05	79 ± 21	102 ± 10	152 ± 13	2 ± 4
± 0.00	88 ± 25	127 ± 11	204 ± 14	0 ± 10
-0.05	102 ± 19	139 ± 12	226 ± 15	5 ± 4

Another source for systematic uncertainty is the arbitrariness of the background model. To evaluate the impact of the background model on the significance a different background model is tested. We use a Landau function to fit the flavour symmetric background and compare the outcome of the fit.

To evaluate the impact of theoretical uncertainties on the cross-section of the background processes each sample has been scaled by $\pm 10\%$. The impact of this variation is found to be negligible since the dominant background is SUSY itself at LM0. Other sources for systematic uncertainties (e.g. luminosity) have not been taken into account because the background is measured directly from data.

To include systematic uncertainties due to the efficiency measurement we include the uncertainties of background model in the likelihood calculation including all correlations. We perform 1000 pseudo experiments and quote the mean of the observed significance including systematic uncertainties.

For the counting experiment an additional source for systematic uncertainties is the efficiency determination which is taken into account in the uncertainty of the extrapolation factor τ. The uncertainty on the extrapolation factor is assumed conservatively to be 20%.

Table 5: Integrated luminosity needed to obtain a significance above 5 σ including systematic uncertainties for both methods.

	σ_{Shape}	σ_{Count}
LM0	200 pb^{-1}	250 pb^{-1}
LM1	250 pb^{-1}	400 pb^{-1}
LM9	350 pb^{-1}	600 pb^{-1}

The luminosities required to obtain a discovery including systematic uncertainties at all three benchmark points are listed in Tab. 5. Including shape information an earlier discovery at each of the points is possible.

5.5 Systematic uncertainty on the endpoint

To evaluate the systematic uncertainty on the dilepton invariant mass endpoint the same uncertainty on the jet energy scale as in Sec. 5.4 is assumed. Additionally an electron energy scale uncertainty of 0.3% is assumed.

To evaluate the uncertainty due to the resolution model we varied the measured resolution by 30% to test the robustness of the model. The impact of the uncertainty in the efficiency measurement has been tested. For both electrons and muons the efficiency is scaled depending on the lepton p_T from $\pm 20\%$ at 10 GeV to $\pm 5\%$ at 100 GeV. The impact of these variations on the dilepton endpoint is displayed in Tab. 6. To evaluate these numbers the full statistics of the sample has been used to minimize a potential statistical bias.

Table 6: Systematic uncertainties on the determination of the dilepton endpoint $m_{ll,max}$.

Variation	Nominal	+ Var.	-Var.
Jet energy scale	51.3 ± 1.5	50.9 ± 1.4	51.3 ± 1.5
Electron energy scale	51.3 ± 1.5	51.0 ± 1.7	51.3 ± 1.3
Resolution model	51.3 ± 1.5	51.1 ± 2.1	51.0 ± 1.4
Muon Efficiency	51.3 ± 1.5	51.3 ± 1.4	51.0 ± 1.8
Electron Efficiency	51.3 ± 1.5	51.2 ± 1.2	51.6 ± 1.1
Background model	51.3 ± 1.5	50.7 ± 1.8	-
Lepton acceptance	51.3 ± 1.5	51.2 ± 1.2	-

5.6 Higher integrated luminosity

At the benchmark points LM1 and LM9 a higher integrated luminosity is necessary to measure the endpoint. Nevertheless the points can be discovered already at an integrated luminosity below 500 pb^{-1}.

The fit of the invariant mass distribution at LM9 using an integrated luminosity of 1 fb^{-1} is shown in Fig. 3(a). The fit to the full MC dataset (10 fb^{-1}) yields a value of

$$m_{ll,max} = \left(62.8 \pm 1.4_{stat.} \pm 0.8_{syst.}\right) \text{ GeV}. \tag{15}$$

The theory value of $m_{ll,max} = 62.9$ GeV is reproduced within the error.

At LM1 a triangle is used as signal model and the fit of the invariant mass distribution at LM1 is shown in Fig. 3(b). The fit to the full MC datset (10 fb^{-1}) yields a value of

$$m_{ll,max} = \left(77.3 \pm 0.9_{stat.} \pm 0.9_{syst.}\right) \text{ GeV}. \tag{16}$$

The theoretical endpoint of $m_{ll,max} = 78.1$ GeV is reproduced within the error. The systematical error in both cases is evaluated as for LM0 in Sec. 5.5.

At LM0 the fit to the invariant mass distribution using an integrated luminosity of 1 fb^{-1} is shown in Fig. 3(c). It yields a value of

$$m_{ll,max} = \left(51.3 \pm 0.7_{stat.} \pm 0.9_{syst.}\right) \text{ GeV}. \tag{17}$$

One can see that the used approximation (neglecting the sfermion exchange) breaks down since the theoretical value is slightly underestimated although quality of the fit is still good.

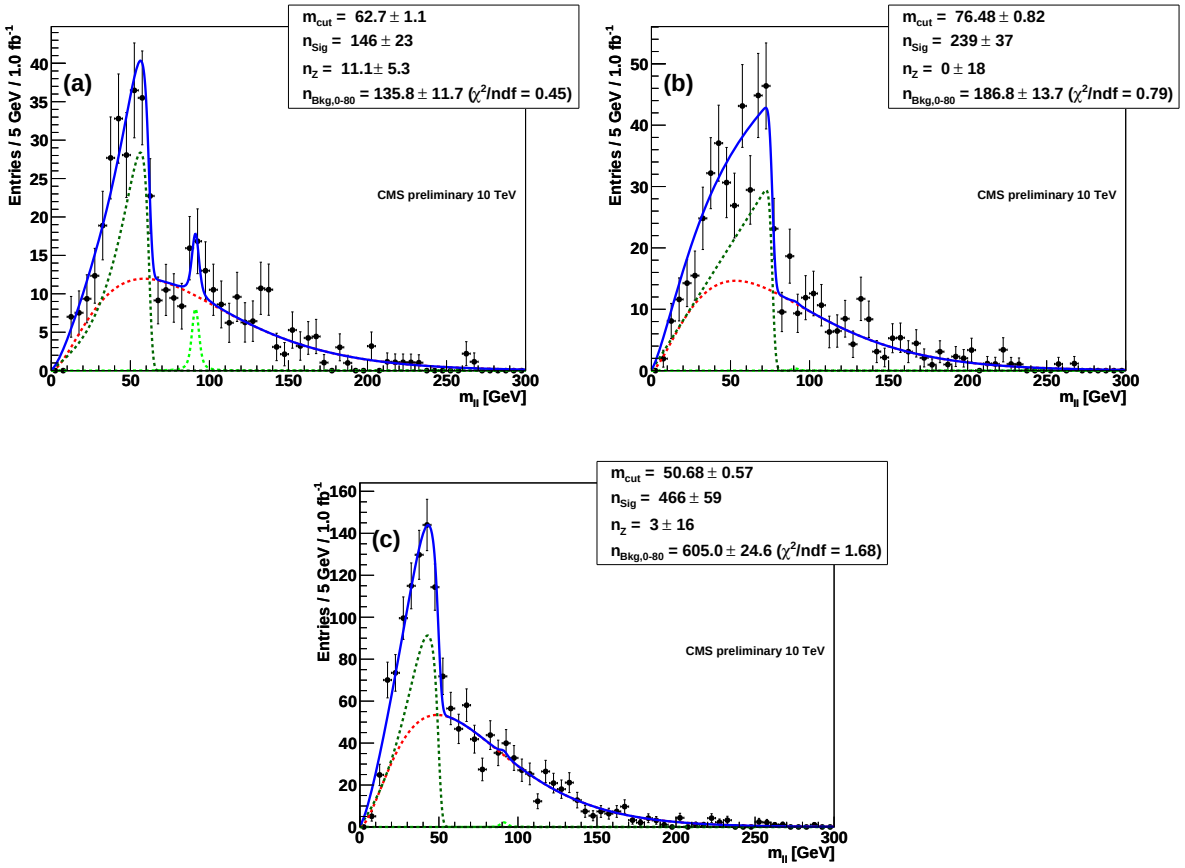

Figure 3: Final fits to the opposite sign same flavour invariant mass distribution at LM9 (a) where the signal model consists of the 3-body model, at LM1 (b) where the signal model is a triangle and at LM0 (c), for 1 fb^{-1}.

6 Conclusion

A significant excess of SUSY opposite sign same flavour lepton pairs can be found within the first 200 pb^{-1} at LM0. The signal provides a quite robust signature and the background determination directly from data is possible. Including systematic uncertainties a significance above $5\,\sigma$ using shape information can be achieved with 200 pb^{-1} of data. From pure event counting a significance of $5\,\sigma$ can be reached with 250 pb^{-1}.

At the other studied benchmark points we observe a needed integrated luminosity to obtain a $5\,\sigma$ discovery using shape information of 250 pb^{-1} (LM1) and 350 pb^{-1} (LM9). The needed amount of data using only the number of observed events yields a value of 400 pb^{-1} for LM1 and 600 pb^{-1} for LM9, respectively.

We presented an unbinned maximum likelihood fit to the dilepton invariant mass distribution (corrected for the difference in muon and electron reconstruction efficiency) with a data-driven resolution determination. At LM0 the combined fit of the dileptonic endpoint is possible with 200 pb^{-1}. We obtain a value of

$$m_{ll,max} = \left(51.3 \pm 1.5_{stat.} \pm 0.9_{syst.}\right)\ \text{GeV}, \tag{18}$$

compared to a theoretical value of 52.7 GeV.

The main main challenge will be the interpretation of such an endpoint since one is not able to distinguish statistically between two- and three-body decay using 200 pb^{-1} of data.

At the benchmark points LM9 and LM1 the endpoint can be measured with an integrated luminosity of 1 fb^{-1}.

References

[1] B. C. Alanach, "SOFTSUSY: a program for calculating supersymmetric spectra," *Comput.Phys.Commun.* **143** (2002) 305–331.

[2] A. Djouadi et al., "Decays of Supersymmetric Particles: the program SUSY-HIT (SUspect-SdecaY-Hdecay-InTerface)," *ActaPhys.Polon.B* **38** (2007) 635–644.

[3] T. Sjostrand et al., "PYTHIA 6.4 Physics and Manual," *JHEP* **0605:026** (2006).

[4] W. Beenakker et al., "Squark and Gluino Production at Hadron Colliders," *Nucl.Phys.B* **492** (1997) 51–103.

[5] M. M. Nojiri and Y. Yamada, "Neutralino decays at the CERN LHC," *Phys.Rev.D* **60** (1999), no. 015006,.

[6] **CMS** Collaboration, "Study of the Z production in association with jets in proton-proton collisions at $\sqrt{s} = 10$ TeV with the CMS detector at the CERN LHC," *CMS Physics Analysis Summary* **JME-08-006** (2008).

[7] J. Alwall et al., "MadGraph/MadEvent v4: The New Web Generation," *JHEP* **0709:028** (2007).

[8] M. Cacciari et al., "Updated predictions for the total production cross sections of top and of heavier quark pairs at the Tevatron and at the LHC," *JHEP* **0809:127** (2008).

[9] S. Frixione and M. L. Mangano, "How accurately can we measure the W cross section?," *JHEP* **0405:056** (2004).

[10] E. James et al., "Muon Identification in CMS," *CMS Note* **2006/010** (2006).

[11] S. Baffioni et al., "Electron Reconstruction in CMS," *CMS Note* **2006/040** (2006).

[12] G. P. Salam and G. Soyez, "A practical Seedless Infrared-Safe Cone jet algorithm," *JHEP* **0705:086** (2007).

[13] **CMS** Collaboration, "Plans for Jet Energy Corrections at CMS," *CMS Physics Analysis Summary* **JME-07-002** (2007).

[14] **CMS** Collaboration, "$\not\!\!E_T$ performance in CMS," *CMS Physics Analysis Summary* **JME-07-001** (2007).

[15] **CMS** Collaboration, "Measuring Electron Efficiencies at CMS with Early Data," *CMS Physics Analysis Summary* **EGM-07-001** (2007).

[16] **CMS** Collaboration, "Dilepton + Jets + MET channel : Observation and Measurement of $\tilde{\chi}_2^0 \to \tilde{\chi}_1^0 ll$," *CMS Physics Analysis Summary* **SUS-08-001** (2008).

[17] U. de Sanctis et al., "Perspectives for the detection and measurement of Supersymmetry in the focus point region of mSUGRA models with the ATLAS detector at LHC," *Eur.Phys.J.C* **52** (2007) 743–758.

[18] W. Verkerke and D. Kirkby, "The RooFit toolkit for data modeling," *arXiv:physics/0306116* (2003).

[19] R. D. Cousins et al., "Evaluation of three methods for calculating statistical significance when incorporating a systematic uncertainty into a test of the background-only hypothesis for a Poisson process," *Nucl.Inst.A* **595** (2008) 480–501.

A Signal decay

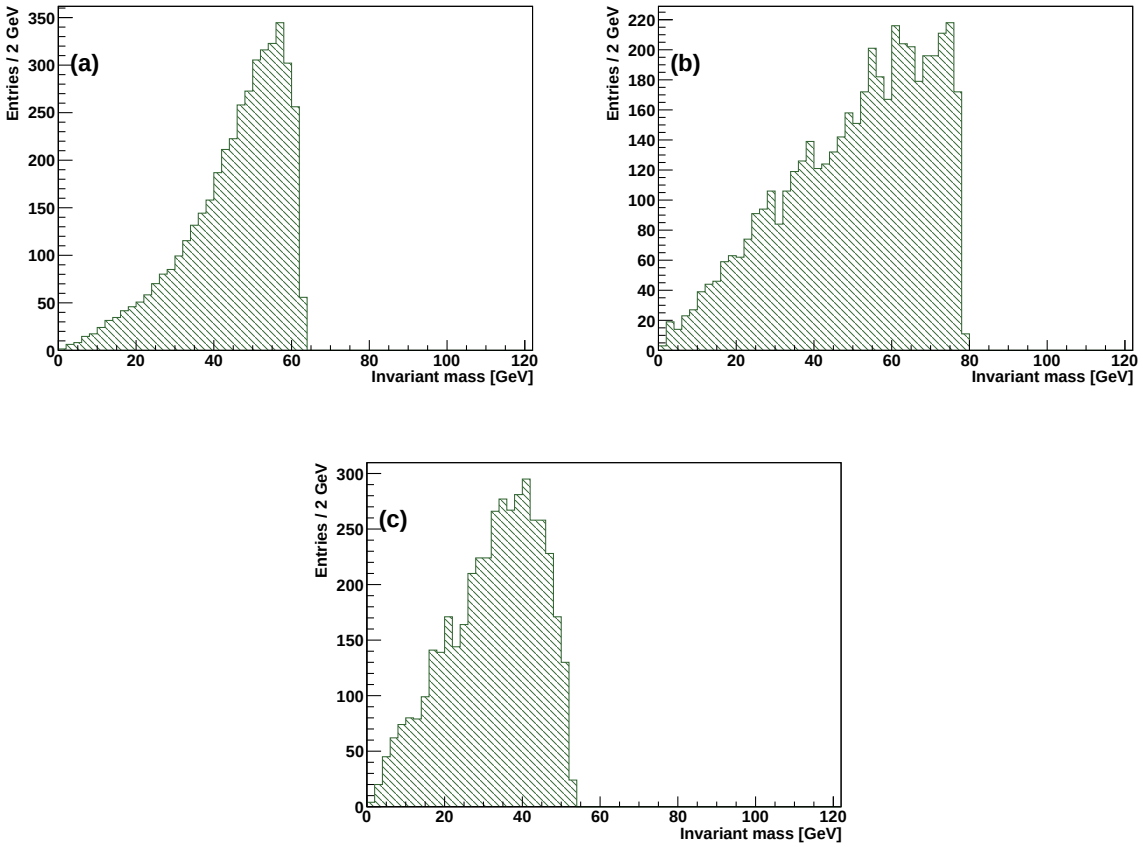

Figure 4: The invariant mass distribution of lepton pairs originating from signal decays in case of the 3-body decay at LM9 is shown in (a). The triangular shaped invariant mass distribution of lepton pairs in case of a 2-body decay at LM1 is shown in (b). The invariant mass distribution at LM0 (3-body decay) is shown in (c).

B Lepton isolation

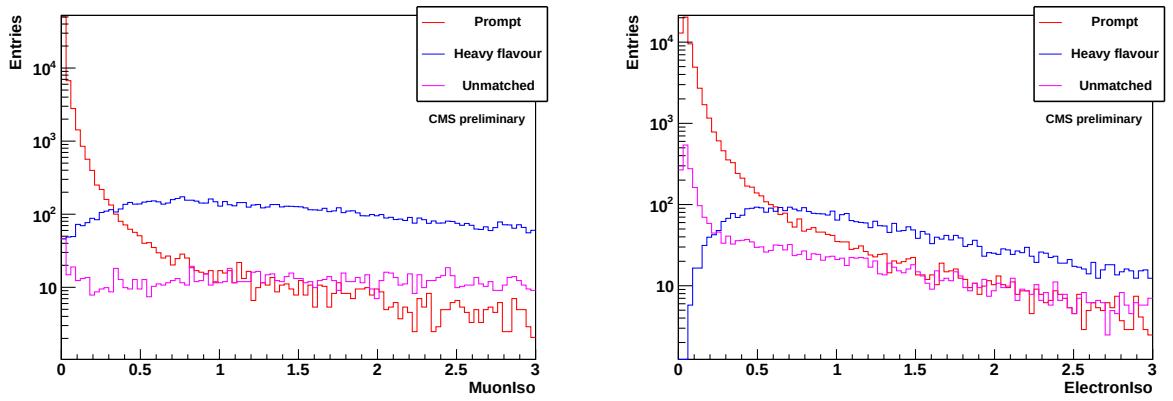

(a) (b)

Figure 5: Isolation value for muons (a) and electrons (b) passing the acceptance and identification cuts in $t\bar{t}$ and SUSY LM0 events. The red curve shows all leptons which can be matched onto a prompt lepton. The blue curve represents leptons matched onto leptons from decays of heavy resonances. Magenta are unmatched leptons, e.g. fake leptons from jets.

C Resolution measurement

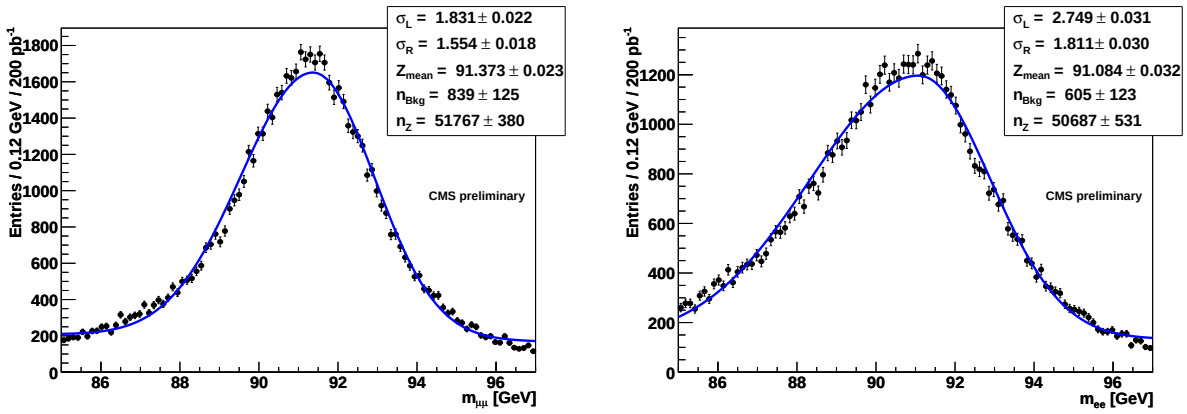

(a) (b)

Figure 6: Resolution measurement from Z events for muons (a) and electrons (b).